Physics Letters A 375 (2011) 2171–2175

Contents lists available at ScienceDirect

Physics Letters A

www.elsevier.com/locate/pla

ZnO-CNT composite nanotubes as nanoresonators

Cheng-Yuan Wang *, Sonipon Adhikari

College of Engineering, Swansea University, Singleton Park, Swansea, Wales SA2 8PP, UK

ARTICLE INFO

Article history:
Received 28 January 2011
Received in revised form 14 April 2011
Accepted 18 April 2011
Available online 29 April 2011
Communicated by R. Wu

ABSTRACT

This Letter reports the very first vibration analysis of the novel composite nanotubes (NTs) synthesized by coating carbon nanotubes (CNTs) with piezoelectric zinc oxide (ZnO). Timoshenko beam theory was used and modified to account for the interlayer van der Waals (vdW) interaction in the inner CNT and hybrid structures of the NTs. The distinctive vibration behaviours of the NTs were captured and the physics behind these unique features was investigated in terms of the critical role of the vdW interaction and the effect of the ZnO coating layer on the structural rigidity of the NTs. The composite NTs are found to be promising for gigahertz/terahertz electromechanical nanoresonators whose frequency can be even higher than that of the core CNTs.

1. Introduction

Nanoscale zinc oxide (ZnO) is a semiconducting material with a wide band gap of 3.37 eV and a large excitation binding energy of 60 meV. Its non-central symmetric wurtzite structure leads to high piezoelectricity of ZnO. These properties and their coupling effects have a wide range of application in optics, optoelectronics, sensors/actuators, spintronics and the new field of nanopiezotronics (e.g., nanogenerators) [1,2]. In contrast to toxic carbon nanotubes, ZnO is bio-safe and biocompatible, which opens the door to the application of ZnO in biomedicine/bio-nanotechnology. ZnO nanostructures can be obtained in a variety of configurations, such as nanowires (NWs), nanobelts, nanoribs, nanohelixes and nanotubes [1,2]. Recently, ZnO-CNT nanocomposites have been fabricated by coating carbon nanotubes (CNTs) with a coaxial and uniform ZnO layer [3–6]. The thickness of ZnO layer can be adjusted by changing the experiment conditions. The synergic of CNTs and ZnO is expected to create exceptional mechanical, electrical and electromechanical properties that cannot be achieved by CNTs and ZnO nanowires (NWs) individually. For example, CNTs can facilitate the charge transfer and promote the charge transport in the composite [4,5] and substantially enhance its structural stiffness. Significant enhancement of secondary electro emission was also achieved by combining ZnO and CNTs [4]. The design of ZnO-CNT nanocomposites provides an important strategy to develop fundamental nanodevices with improved performance and an enlarged range of applications in nanotechnology, such as high frequency electromechanical nanoresonators, electromechanically coupled biosensors (actuators) with high selectivity and sensitivity, reinforcing fibres in composites and piezoelectric nanogenerators.

The synthesis of these novel nanocomposites has excited significant interest in their fundamental physical and chemical properties. Existing works on the physical behaviours are mainly focused on the electronic properties [4–6]. The mechanical properties of ZnO-CNT nanotubes however have not received enough attentions so far. It is thus of great interest to initiate a series of study on the mechanics of ZnO-CNT nanocomposites. In particular, similar to the cases of CNTs and various NWs [7–10], the vibration of such nanocomposites is essential for their applications in nanotechnology and thus, forms one of the major concerns in nanomechanics. Specifically, the hybrid structures of the nanocomposites would lead to unique vibrational behaviours qualitatively different from those of individual CNTs and ZnO NWs. Furthermore, size-dependence of elastic modulus or surface effect was captured for ZnO NWs [11,12], which distinguishes them from bulk ZnO. These small scale effects on mechanical properties has become a current topic of great interest for ZnO nanostructures and certainly deserve to be examined for the CNT-ZnO nanocomposites when crystalline ZnO coating layer is achieved.

Motivated by these ideas, we investigated the transverse vibrations of the ZnO-CNT nanocomposites. The analysis was conducted by using a multilayer beam model developed by modifying single Timoshenko beam model to account for the hybrid structures of the nanocomposites and the van der Waals (vdW) interaction in the core CNT. Particular attention is paid to the dependence of vibration frequency and vibration modes on the thickness of the ZnO coating layer and the interlayer vdW interaction of the core CNT. The physics of the observed phenomena was also discussed in details to bring in an in-depth understanding of the unique behaviours. It is expected that the obtained models and

* Corresponding author. Tel.: +44 (0) 1792 602825.
E-mail address: chengyuan.wang@swansea.ac.uk (C.-Y. Wang).

0375-9601/$ – see front matter © 2011 Published by Elsevier B.V.
doi:10.1016/j.physleta.2011.04.031

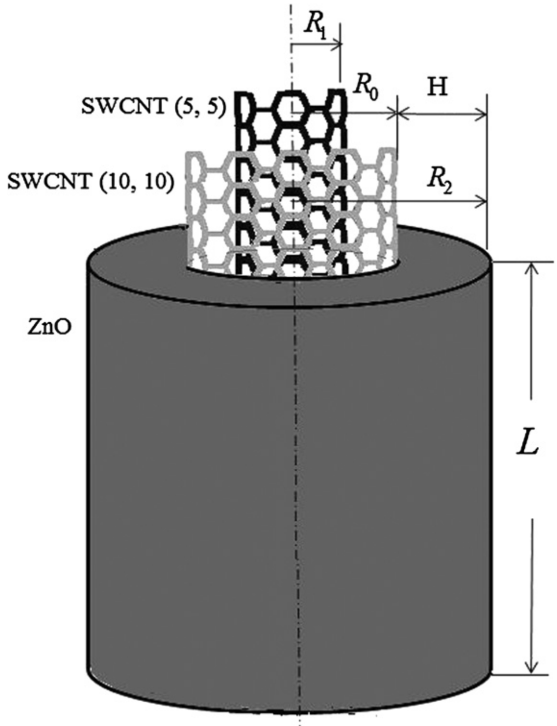

Fig. 1. The structure of the ZnO-DWCNT composite nanotubes.

numerical results can facilitate the study on other composite nanotubes made by coating CNTs with SiOx or various metallic materials.

2. Multilayer-beam model

2.1. Structures of ZnO-CNT composite nanotubes

To study the transverse vibration of the ZnO-CNT nanotubes (NTs) we consider an example NT consisting of a core double-walled CNT (DWCNT) $(5,5)@(10,10)$ and an outer concentric ZnO coating layer (Fig. 1). As shown in Fig. 1, the hybrid nanostructure comprises two nanobeams. (1) Beam 1 is a singlewalled carbon nanotube (SWCNT) $(5,5)$ of the core DWCNT. (2) Beam 2 is a composite beam comprising the ZnO coating layer and a SWCNT $(10,10)$. Here the ZnO-SWCNT interface could play a significant role in the composite beam 2, and thus needs to be handled carefully in the modelling work. To our best knowledge, the structure of ZnO-SWCNT interface is only examined in [5]. In this work it is shown that the covalent bond is introduced between ZnO and SWCNT via ultrasonic processing with acid-treated SWCNTs, zinc acetate, and triethanolamine [5]. Thus, in our analysis a perfect bonding is assumed at the ZnO-SWCNT interface. On the other hand, in Ref. [5] the ZnO layer with poor crystallinity is obtained at low temperature 95 °C for the composite NTs. These features substantially reduce the residual stresses at the interface, which could be otherwise much higher due to the difference in thermal expansion coefficients and the lattice constants of the two sides of the interface. Thus such an interface stress will be neglected in our analysis. (3) In addition, beams 1 and 2 are separated by 0.34 nm before vibration (i.e., the interlayer spacing of the DWCNT) and the vibrations of the two beams are coupled via the interbeam van der Waals (vdW) interaction.

2.2. Vibration analysis of ZnO-CNT composite nanotubes

In the present study, beam 1 and beam 2 of the composite NT are treated as two Timoshenko beams which have circular cross sections. They are subjected to a distributed transverse force due to the vdW interaction between them. The dynamic equations of the composite NTs can thus be written as follows [13–15].

$$\begin{cases} -(GA)_i k\left(\dfrac{\partial \varphi_i}{\partial x} - \dfrac{\partial w_i}{\partial x^2}\right) + p_i(x) = (\rho A)_i \cdot \dfrac{\partial^2 w_i}{\partial t^2} \\ (EI)_i \dfrac{\partial^2 \varphi_i}{\partial x^2} - (GA)_i k \cdot \left(\varphi_i - \dfrac{\partial w_i}{\partial x}\right) = (\rho I)_i \cdot \dfrac{\partial^2 \varphi_i}{\partial t^2} \end{cases} \quad (1)$$

where $i = 1$ and 2 represents the quantities of beams 1 and 2, respectively. w_i and φ_i are transverse deflection and rotation angle; $k(=0.8)$ is the shear coefficient; $(EA)_i$, $(EI)_i$ and $(GA)_i$ are extensional rigidity, bending rigidity and shear rigidity, respectively; $(\rho A)_i$ and $(\rho I)_i$ are mass density per unit length and mass moment of inertia [13–15]. In addition, $p_i(x)$ is the transverse force on the two beams due to the interbeam vdW interaction, where $p_1(x) = c(w_1 - w_2)$ and $p_2(x) = -c(w_1 - w_2)$. The interlayer vdW interaction coefficient c is defined by [13]

$$c = \frac{320(2R_1)\ \text{erg/cm}^2}{1.6d^2}, \quad d = 0.142\ \text{nm} \quad (2)$$

Here R_1 is the radius of beam 1, i.e., the SWCNT $(5,5)$ of the core DWCNT. Substituting $w_i = A_i \cdot \sin(x\pi/L) \cdot e^{i\omega t}$ and $\varphi_i = \Phi_i \cdot \cos(x\pi/L) \cdot e^{i\omega t}$ into Eq. (1) for simply supported composite NTs yields algebraic equations $M(\omega)_{4\times4} \cdot [A_1 \quad \Phi_1 \quad A_2 \quad \Phi_2]^T = 0$. Here A_i and Φ_i $(i = 1, 2)$ are transverse and shear vibration amplitudes, ω is angular frequency, t is time, L is the length of the NT and M is a coefficient matrix. The condition for nonzero solution of $[A_1 \quad \Phi_1 \quad A_2 \quad \Phi_2]$ reads

$$\det M(\omega)_{4\times4} = 0 \quad (3)$$

Solving Eq. (3) one can obtain the vibration frequency $f = \omega/2\pi$. The associated amplitude ratio W_1/W_2 can be calculated by

$$\begin{aligned} \frac{W_1}{W_2} = {} & \left(\left[k \cdot (GA)_2 (m\pi/L)\right]^2 \right. \\ & - \left[(\rho A)_2 \omega^2 - k \cdot (GA)_2 (m\pi/L)^2 - c\right] \\ & \cdot \left.\left[(\rho I)_2 \omega^2 - (EI)_2 (m\pi/L)^2 - k \cdot c(GA)_2\right]\right) \\ & /\left(c \cdot \left[(\rho I)_2 \omega^2 - (EI)_2 (m\pi/L)^2 - k \cdot (GA)_2\right]\right) \end{aligned} \quad (4)$$

2.3. Calculation of structural parameters

For beam 1, i.e., SWCNT $(5,5)$ as a hollow beam with mean radius $R_1 = 0.34$ nm, five parameters $(EA)_1$, $(EI)_1$, $(GA)_1$, $(\rho A)_1$, $(\rho I)_1$ in Eq. (1) can be calculated by using classical formulae shown in [11–13] and equivalent Young's modulus $E_{cnt} = 3.5$ TPa, effective thickness $h = 0.1$ nm, mass density per unit lateral area $\rho_{cnt} = 2.27\ \text{g/cm}^3 \times 0.34$ nm, Poisson ratio $\nu_{cnt} = 0.2$ [16,17] and radius R_1.

For beam 2, i.e., composite beam consisting of the ZnO coating layer and SWCNT $(10,10)$, five parameters $(EA)_2$, $(EI)_2$, $(GA)_2$, $(\rho A)_2$, $(\rho I)_2$ represented by $(Q)_2$ are given by

$$(Q)_2 = (Q)_{zno} + (Q)_{swcnt(10,10)} \quad (5)$$

where $(Q)_{zno}$ and $(Q)_{swcnt(10,10)}$ denote the above five quantities of (1) the ZnO layer (a hollow beam of outer radius R_2 and inner radius R_0) and (2) SWCNT $(10,10)$ (a hollow beam with mean radius $R_0 = 0.68$ nm) (see Fig. 1). $(Q)_{swcnt(10,10)}$ is obtained by following the procedure demonstrated for beam 1 and radius R_0, and $(Q)_{zno}$ is calculated via classic formulae [11–13] and Young's modulus $E_{zno} = 140$ GPa [11,12], the mass density $\rho_{zno} = 5.61\ \text{g/cm}^3$ [18] and the thickness $H(= R_2 - R_0)$ of the ZnO layer (Fig. 1). In addition, shear modulus G_{zno} is estimated based on the classical relation between E_{zno} and G_{zno}. Here it should be pointed out that the elastic properties of the non-crystalline ZnO layer are not available in literature. Thus the value of crystalline ZnO $E_{zno} = 140$ GPa is used as an approximation in this initial study, which should be higher than that of ZnO with poor crystallinity. The results based on this value thus would over estimate the frequency of the NTs to some extend but the tendency and major physics will be captured based on the present model.

3. Results and discussion

Following the above methods, we have investigated transverse vibrations of the ZnO-DWCNT composite NTs. In-phase and out-of-phase vibrations are achieved, where beams 1 and 2 of the NTs oscillate in the same and opposite directions, respectively. The out-of-phase mode exhibits frequency higher than that of in-phase mode. In what follows two major issues shown below will be examined to capture the distinctive vibration behaviours of the NTs and investigate the physics behind these unique features.

3.1. Dependence of vibration on the ZnO coating layer

In this section we first study the dependence of the in-phase mode on the thickness of the ZnO layer. The frequency f_1 of the in-phase mode is presented in Fig. 2 where the length L of the NT is fixed at 60 nm and the thickness H of its ZnO layer rises from zero (i.e., DWCNT without coating layer) to 25 nm. In this process, the NT transforms from a slender beam to a very stocky beam with aspect ratio $\gamma(=\frac{L}{2R_2}=\frac{L}{2(R_0+H)})$ decreasing from 44 to 1.2. It is noted that for the NTs considered in Fig. 2, f_1 of the in-phase mode rises from one to around 60 gigahertz, i.e., 10^9(Hz) to 6×10^{10}(Hz), when the half axial wave number n increases from 1 to 5. When thin ZnO layer is coated on the core DWCNT (e.g., $H \leqslant 2$ nm) f_1 first decreases rapidly with increasing H and reaches its lowest value at $H \approx 0.73$ nm. Further raising H then up shifts f_1 and at sufficiently large H (e.g., $H \geqslant 2.5$ nm) f_1 becomes even higher than the frequency of the core DWCNT (i.e., $H = 0$). Thus, compared with the DWCNT the ZnO-DWCNT composite NTs can be nanoresonators with much higher frequency. This is a little surprising as it is well known that adding ZnO layer to a DWCNT leads to lower equivalent modulus and larger mass density of the composite NTs. To understand the results in Fig. 2 we calculated amplitude ratio W_1/W_2 of the in-phase mode in Fig. 3. It is seen in Fig. 3 that W_1/W_2 of the in-phase mode is very close to unity for all half wave number n and thickness H considered. This suggests that the transverse deflections of beams 1 and 2 are always equal, i.e., $w_1 = w_2$. Thus the in-phase mode is a collective transverse vibration of both beam 1 and beam 2, and during the vibration there is no relative deflection between them. Such a collective vibration can be attributed to the interbeam vdW interaction which is strong enough to resist change in the spacing between the two beams. In this case, the NT behaves like a single layer hollow beam with bending rigidity $(EI) = (EI)_1 + (EI)_2$ and mass density per unit length $(\rho A) = (\rho A)_1 + (\rho A)_2$. At $H \leqslant 2$ nm such an equivalent beam is thin with the aspect ratio $\gamma > 10$. Thus it can be adequately modelled as an Euler beam whose frequency is determined by the ratio $\alpha(=\sqrt{\frac{(EI)}{(\rho A)}})$, i.e., $f_1 = C\cdot\sqrt{\frac{(EI)}{(\rho A)}}$ (C is a constant) [13]. From here it is clear that, at $H \leqslant 2$ nm the distinctive behaviours of f_1 observed in Fig. 2 is a result of the growth competition between the bending rigidity (EI) and the mass density (ρA) due to increasing thickness H of the ZnO layer. This conclusion has been confirmed in Fig. 4(a) where the tendency of ratio α to change with H is consistent with that of f_1 shown in Fig. 2. Specifically α and f_1 reach their minimum values at the same point, i.e., $H \approx 0.73$ nm. Indeed, raising H of the NT increases its radius, which enhances the moment of inertia and therefore, the bending rigidity (EI) of the NT although its equivalent Young's modulus decreases in the process due to the low modulus of ZnO. Specifically, when the ZnO layer is not very thin, e.g., $H > 0.73$ nm, (EI) rises with H much faster than the area of cross section and thus the mass density per unit length (ρA). As a result α increases substantially with rising H as shown in Fig. 4(a). It follows that the increase of the bending rigidity (EI) due to growing H is responsible for the frequency upshift observed for the in-phase mode at $H > 0.73$ nm (Fig. 2).

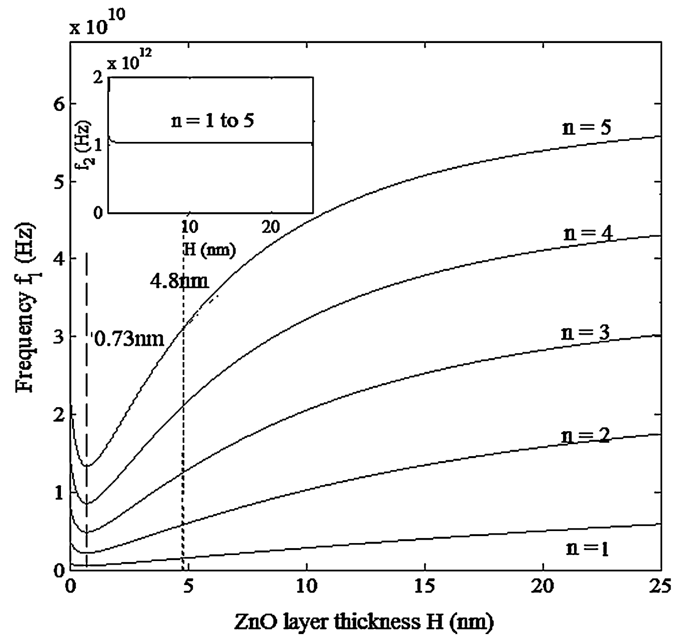

Fig. 2. The frequency f_1 of the in-phase mode against the thickness H of the ZnO layer calculated in two cases, case I: using the modulus of bulk ZnO The frequency f_2 of the out-of-phase mode is obtained in above two cases and shown in the inset.

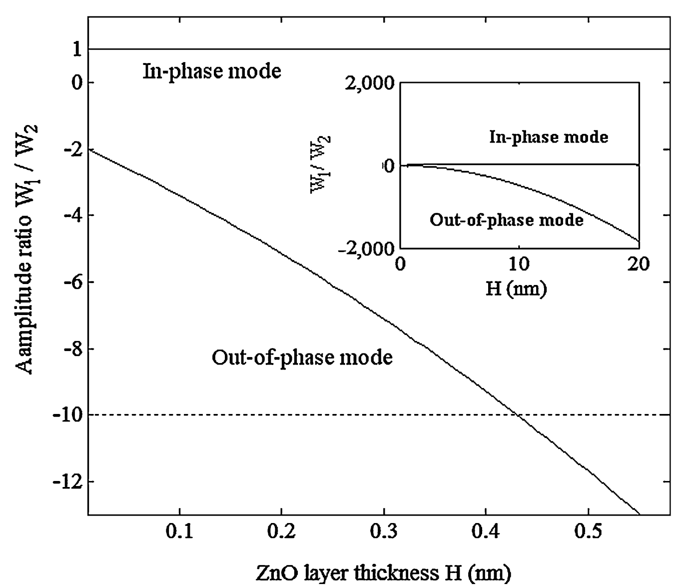

Fig. 3. Amplitude ratios calculated for the in-phase mode and out-of-phase mode of the ZnO-DWCNT composite NTs with the increasing thicknesses H of the ZnO layer.

Further raising H to $H > 2$ nm, the aspect ratio γ of the NT becomes smaller than 10. Thus the NT is converted from an Euler beam into a Timoshenko beam where shear deformation and rotary inertia play an important role in its vibrations. In Fig. 4(b) the ratio $\beta = \frac{(GA)}{(\rho I)}$ of the NTs decreases rapidly with rising H show-

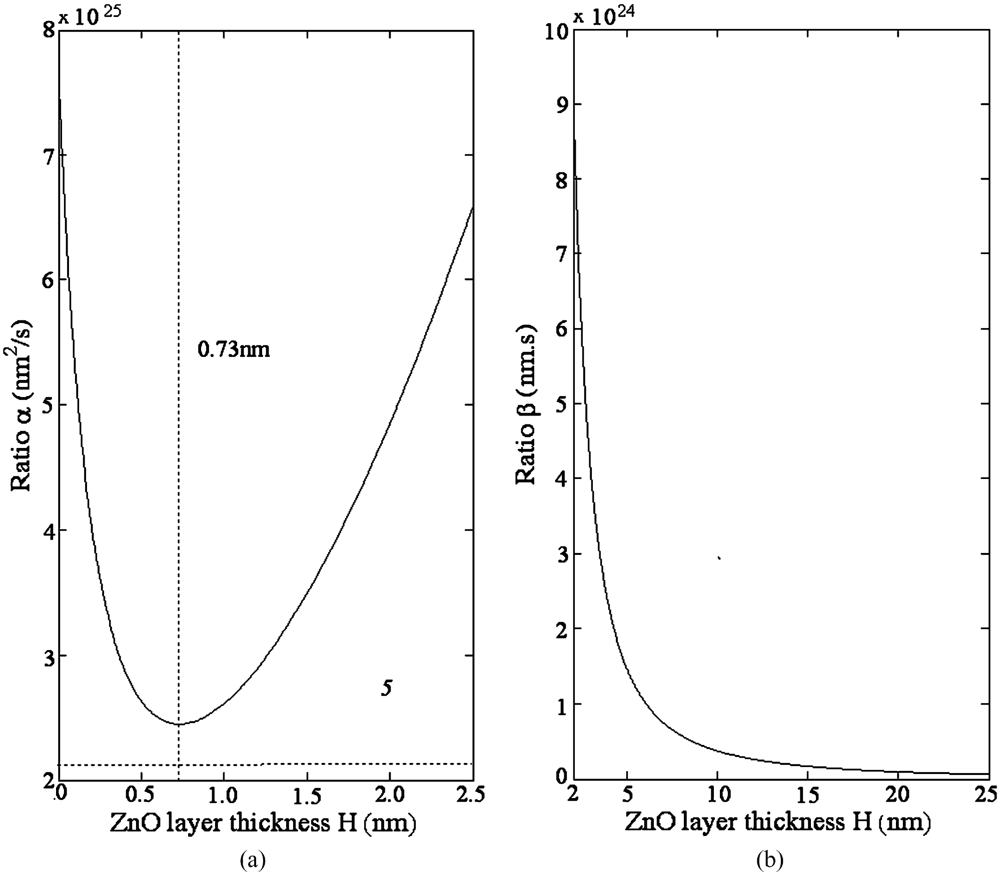

Fig. 4. The tendency of (a) ratio $\alpha(=\sqrt{\frac{(EI)}{(\rho A)}})$ and (b) ratio $\beta(=\sqrt{\frac{(GA)}{(\rho I)}})$ to change with the thickness H of the ZnO layer.

ing that the involvement of (ρI) and (GA) is responsible for the reduced rate of increase observed in Fig. 2 for f_1 at $H > 2$ nm.

3.2. Influence of the vdW interaction

In Section 3.1 we see that the interbeam vdW interaction is strong enough to resist the change in the interbeam spacing during the in-phase vibration of the composite NTs. Next let us examine the effect of this vdW interaction on the out-of-phase mode. As shown in the inset of Fig. 2, the frequency f_2 of the out-of-phase mode is of the order 1 terahertz and is almost a constant independent of half wave number n and the ZnO coating thickness H (see inset of Fig. 2). In Fig. 3, we calculated the amplitude ratio W_1/W_2 of the out-of-phase mode. The figure shows that W_1/W_2 of the out-of-phase mode is insensitive to the variation of n but its magnitude $|W_1/W_2|$ grows considerably with rising H. When H exceeds 0.5 nm the magnitude of W_1 is 10–1000 time that of W_2. Thus, contrary to the in-phase mode which is a collective vibration of beams 1 and 2, the out-of-phase mode is basically the transverse vibration of beam 1, i.e., the inner SWCNT $(5,5)$, whereas the outer composite beam 2 is not significantly involved in the vibration when the ZnO layer is not very thin, e.g., $H > 0.5$ nm. This explains why frequency f_2 is insensitive to the variation of the ZnO thickness H. It is worth mentioning here that since ZnO layer does not exert significant influence on the out-of phase vibration the frequency of this vibration is almost independent of the value of Young's modulus used for ZnO in analysis. In addition, the analysis of amplitude ratio also implies that through the interbeam vdW interaction a very small vibration deflection of outer beam 2 can excite the terahertz vibration of the inner SWCNT with a deflection up to three orders of magnitude larger. Specifically it is noted that nanoscale ZnO exhibits piezoelectricity, which makes the composite NTs promising for electromechanical nanoresonators of high or ultrahigh frequency.

Here the out-of-phase vibration is basically the transverse vibration of the inner SWCNT $(5,5)$. In the inset of Fig. 2, such a transverse vibration of the SWCNT exhibits terahertz frequency which does not change with half wave number n. This behaviour is in sharp contrast to the transverse vibration of an isolated SWCNT $(5,5)$ (length 60 nm), where the frequency, as we calculated, is of the order of gigahertz ($\sim 10^9$ Hz) and increases substantially with growing n. The discrepancy between the core SWCNT and an isolated SWCNT can be attributed to the vdW interaction between the core SWCNT $(5,5)$ (i.e., the inner beam 1) and outer beam 2, which largely controls the transverse vibration of the SWCNT $(5,5)$ and up shifts its frequency by three orders of magnitude to terahertz (10^{12} Hz). The deformation strain of the SWCNT $(5,5)$ however does not affect the vibration frequency significantly. As a result, the variation of n cannot exert visible influence on frequency f_2. In other words, during the vibration the deformation energy of the core SWCNT $(5,5)$ is negligible as compared with the potential energy between beams 1 and 2. This observation shows that the vdW interaction can play a predominant role in reshaping the mechanical behaviours of nanostructures/nanomaterials.

Furthermore, we noted that for radial breathing mode of SWCNTs the intertube vdW interaction can only raise the frequency (~ 175 cm^{-1} or 5×10^{12} Hz) of isolated SWCNTs $(9,9)$ or $(10,10)$ by 6–14 cm^{-1}, i.e., less than 10% [19,20]. Here it is easy to understand that the frequency of an isolated SWCNT measures its structural rigidity for the specific deformation patterns. Thus, the radial rigidity of isolated SWCNTs $(9,9)$ or $(10,10)$ controlling a terahertz radial breathing vibration is much higher than the bending rigidity of a long SWCNT (5, 5) associated with a gigahertz transverse vibration. This comparison shows that the influence of the vdW interaction on the mechanics of a nanostructure depends sensitively on the specific structural rigidity that governs the corresponding deformation. This influence can be predominant in the nanostructures of a very low structural rigidity.

Here it should be pointed out that the ZnO-SWCNT interface could be of different nature depending on the experimental techniques used in the fabrication of the composite NTs. Thus in some cases, particularly if the crystalline ZnO layer can be obtained, the interface stress could be strong enough to exert significant influence on the overall vibration behaviours of the composite NTs. This issue indeed needs to be addressed in the future study when more experimental data are available. On the other hand, in addition to ZnO-CNT composite NTs, SiOx-CNT, Cu-CNT, Ni-CNT and W-CNT composite NTs of similar structures have also been synthesized successfully. The results of the present study thus can provide useful guidance for the further research on the vibration of these composites NTs.

4. Conclusions

Transverse vibration is investigated for the composite NTs fabricated by coating a DWCNT (5, 5)@(10, 10) with ZnO nanocrystals. The analysis is carried out based on Timoshenko beam theory. The in-phase and out-of-phase modes are achieved and the effects of the ZnO coating layer and the interbeam vdW interaction are examined in details. The new findings are summarized as follows:

(1) The in-phase mode of the NTs is a collective vibration of their two constitutive beams. Its frequency first decreases with increasing thickness H of ZnO layer and reaches its lowest value at $H \approx 0.73$ nm. It then rises rapidly with growing thickness H. This distinct behaviour is due to the rising H-induced growth competition between the bending stiffness and mass density (per unit length) of the NTs. Further raising H leads to lower rate of frequency increase as a result of the involvement of the shear deformation and rotary inertia of the NTs.

(2) The out-of-phase is a terahertz transverse vibration primarily of the inner SWCNT (5, 5). The vdW interaction in the NTs controls the transverse vibration of the SWCNT (5, 5) and up shifts its frequency by three orders of magnitude. The half wave number n related to deformation energy, however, does not have observable influence on the vibration. These behaviours are in sharp contrast to those of individual SWCNTs and shows that the vdW interaction can play a predominant role in the mechanics of nanostructures.

References

[1] Z.L. Wang, Mater. Sci. Eng. R 64 (2009) 33.
[2] Y.J. Xing, Z.H. Xi, X.D. Zhang, J.H. Song, R.M. Wang, J. Xu, Z.Q. Xue, D.P. Yu, Solid State Commun. 129 (2004) 671.
[3] L. Huang, S.P. Lau, H.Y. Yang, E.S.P. Leong, S.F. Yu, J. Phys. Chem. B 109 (2005) 7746.
[4] L. Huang, S.P. Lau, H.Y. Yang, S.F. Yu, Nanotechnology 17 (2006) 1564.
[5] C.C. Lin, B.T.T. Chu, G. Tobias, S. Sahakalkan, S. Roth, M.L. H Green, S.Y. Chen, Nanotechnology 20 (2009) 105703.
[6] W. Ma, D.B. Tian, Bioelectrochemistry 78 (2010) 106.
[7] A. Husain, J. Hone, H.W.C. Postma, X.M.H. Huang, T. Drake, M. Barbic, A. Scherer, M.L. Roukes, Appl. Phys. Lett. 83 (2003) 1240.
[8] C. Li, T.W. Chou, Appl. Phys. Lett. 84 (2004) 121.
[9] M. Tabib-Azar, M. Nassirou, R. Wang, S. Sharma, T.I. Kamins, M.S. Islam, R.S. Williams, Appl. Phys. Lett. 87 (2005) 113102.
[10] P. Zijlstra, A.L. Tchebotareva, J.W.M. Chon, M. Gu, M. Orrit, Nano Lett. 8 (2008) 3493.
[11] R. Agrawal, B. Peng, E.E. Gdoutos, H.D. Espinose, Nano Lett. 8 (2008) 3668.
[12] M.R. He, Y. Shi, W. Zhou, J.W. Chen, Y.J. Yen, J. Zhu, Appl. Phys. Lett. 95 (2009) 091912.
[13] J. Yoon, C.Q. Ru, A. Mioduchowski, Phys. Rev. B 66 (2002) 233402.
[14] S. Timoshenko, Vibration Problems Engineering, Wiley, New York, 1974.
[15] J.N. Reddy, S.D. Pang, J. Appl. Phys. 103 (2008) 023511.
[16] C.Y. Wang, L.C. Zhang, Nanotechnology 19 (2008) 195704.
[17] R.C. Batra, S.S. Gupta, J. Appl. Mech. ASME 75 (2008) 061010.
[18] Website: http://en.wikipedia.org/wiki/Zinc_oxide.
[19] D. Kahn, J.P. Liu, Phys. Rev. B 60 (1999) 6535.
[20] U.D. Venkateswaran, A.M. Rao, E. Richter, M. Menon, A. Rinzler, R.E. Smalley, P.C. Eklund, Phys. Rev. B 59 (1999) 10928.